Egypt. J. Geo. **Vol. 69,** pp: 355 - 274 (2025)

Egyptian Journal of Geology

https://egjg.journals.ekb.eg

Integrated Seismic Attributes and Spectral Decomposition for Reservoir Characterization Apollonia Formation Northwest Abu El-Gharadig Basin, Egypt

Mahmoud Shouair Abdellatif Shouair[1], **Mahmoud Yousry Zein El-Din**[1] and **Badr Abbas Khalil** [2]

1 *Geology Department, Faculty of Science, Al Azhar University, Cairo, Egypt.*

2 *HBS International Egypt LTD, Cairo, Egypt*

THIS PAPER attempts optimum utilization of studied field resources by evaluating the previously under-explored unconventional Apollonia chalky carbonate reservoir petrophysically characterized very high drilling gas readings while the deep resistivity maximum 3 ohm due to the content of irreducible water very high ranges from 40-80% based on core data generally our reservoir petrophysically characterized by high porosity between 12-45% with average 32% and very low permeability maximum 1.5 mD that need further stimulation operations (acidizing and hydraulic fracturing). This work discussed the structural pattern and fault distribution of the study area to understand the tectonic framework that controlled the Apollonia-A Formation. Several normal faults had been unravelled through seismic data interpretation that influenced the geometry and compartmentalization of the studied reservoir. In this respect, seismic attributes and spectral decomposition techniques were integrated to enhance subsurface interpretation, presenting reliable tools for reservoir characterization. Amplitude, coherence, and curvature seismic attributes have been applied for delineating structural and stratigraphic features, while spectral decomposition allowed for the identification of thin beds and frequency anomalies related to gas-bearing zones. Integration of the above techniques provided a detailed and high-resolution view of the reservoir architecture and heterogeneity. The results highlighted the distribution of gas anomalies and lateral continuity of the reservoir across Apollonia-A Formation, which helped the identification of potential gas-rich zones and an increase in confidence in the delineation of the productive intervals for further exploration and development.

Keywords: RMS Amplitude, Spectral Decomposition, Energy Attributes, Apollonia Formation.

1. Introduction

The Western Desert shows a rather stable shelf setting that is only subject to mild subsidence. However, a series of isolated and spatially limited depocenters occurred along this shelf, leading to the development of several localized sedimentary basins (El-Gawad, Abd, et al., 2021). Northern Western Desert basins are believed to have been developed as a single rifting system, perhaps in the Permo-Triassic period, and subsequently evolved into a pull-apart basin configuration (Bekhiet, M. H., et al., 2011).

The Apollonia unconventional chalky carbonate reservoir (Eocene) belonging to the Abu El-Gharadig Basin which is subsequently confined between Dabaa shale (Oligocene) formation and Khoman carbonate Formation (Senonian). This reservoir is explored by AMOCO in 1970 and drilled two exploration wells WD7-1 and WD7-2 targeting Apollonia but unfortunately, they were a noncommercial production. It is fortunate to note that the first discovery was made by Shell company in 2007 that was highlight the commerciality of such reservoir. (Bassiouni et al., 1982., EGPC, 1992, Shamah et al.,1993; Al Mahdy, 2013, El-Bendary et al., 2016; Sedek; Elmahdy et al., 2018; Kamel and Nagy, 2014; Marzouk, 2002; Salah et al. 2016).

The Apollonia target has been identified as an unconventional reservoir that requires more integrated methods to assess and extract the hydrocarbon

*Corresponding author e-mail: Mahmoud.shouiar@gmail.com

Received: 25/10/2025; Accepted: 21/11/2025

DOI: 10.21608/EGJG.2025.435676.1131

volumes trapped within it. These methods can help determine the structural and lithological features of the reservoir by utilizing additional seismic attributes derived from the seismic wave signals obtained from seismic data (Liner, 2004; Chopra and Marfurt, 2005). A key factor in influencing seismic attributes is the seismic wavelet, which includes its phase, amplitude, and frequency.

To characterize a reservoir, it is essential to assess its structural configuration, stratigraphic distribution, and petrophysical parameters using specialized algorithms that utilize phase information for the interpretation of stratigraphic seismic data by analyzing and evaluating reflector characteristics such as shape, geometry, and continuity. In contrast, the attributes derived from amplitude serve as quantified physical parameters (including velocity, acoustic impedance, reflection coefficient, and absorption effect) to illustrate the structural configuration. Meanwhile, frequency attributes are utilized to assess the properties of the reservoir (Taner, 2001; Brown, 2001; Chopra and Marfurt, 2005).

Much of the seismic exploration work has concentrated on determining the best locations and outlining the shapes of subsurface carbonate formations, such as reefs, which exhibit high porosity and permeability. The reflections at the boundary between grainstone and carbonate mudstone (the porous-nonporous margin) typically have lower reflectivity and resolution than those found in siliciclastic sequences, and interpretation challenges regarding reflector geometries arise due to the diagenetic processes of dissolution and karstification in carbonates (Chopra and Marfurt, 2007). During the lithification process, carbonate rocks behaved as brittle materials, making them more prone to fracturing compared to siliciclastic rocks. In this context, Chopra and Marfurt (2007) indicated that if the original interconnected pores between or within carbonate particles have not been retained, a carbonate reservoir will require an open fracture system to effectively store and produce hydrocarbons.

The data at hand, which includes prior research, 3D seismic information, and well logging results, will be utilized to achieve the primary goal of this study. The main aim of this research is to enhance the comprehension of structure and lithology analysis by utilizing various attributes such as variance, similarity, energy, and RMS amplitude, ultimately leading to a more in-depth understanding. This study has been conducted to facilitate the analysis of potential structural and stratigraphic variability through fast Fourier transform (FFT).

This method enables the visualization of subsurface characteristics. It offers advantages over traditional seismic attributes by delivering frequency content that is essential for structural and stratigraphic analysis, which traditional seismic attributes are unable to provide. Furthermore, this technique provides a more dependable interpretation of stratigraphy and/or direct hydrocarbon indicators (DHI) compared to conventional seismic methods (Fahmy et al. 2005).

2. Geological Setting

The area under investigation (NW Abu El-Gharadig Basin) is lied in the northwestern side of the Western Desert, Egypt between latitudes min: 29.57’18.32"N, max: 29.59'59.04"N and longitudes min: 27.46'35.12"E max: 27.50'56.57"E (Fig.1). Due to the high heterogeneity in carbonate facies and complex styles of structural deformation, the evaluation of the carbonate reservoir is very challenging, because it’s demanded an application of geophysical techniques for figure out the characterization of the carbonate reservoir (Burchette, 2012; Cerepi et al., 2003). (Fig.1).

The Abu El-Gharadig basin showcases various graben or half-graben structures due to a mix of E-W, WNW, ENE, and NNE fractures. This basin stretches 330 km in length and has a width that ranges from 50 to 75 km in an east-west direction, segmented into three uneven areas of sedimentary deposits by ridges that trend NE-SW. NW-SE oriented normal faults intersect these ridges. The structural layout of the Abu Gharadig field includes two primary en`echelon normal faults that trend NE-SW, which formed during the Jurassic to Early Cretaceous periods due to NW-SE extensional forces. Between the Late Cretaceous and Middle Eocene periods, these faults underwent positive structural inversion, leading to the formation of the Abu Gharadig anticline (El Gazzar et al., 2016; Abd El Aal and Moustafa, 1988).

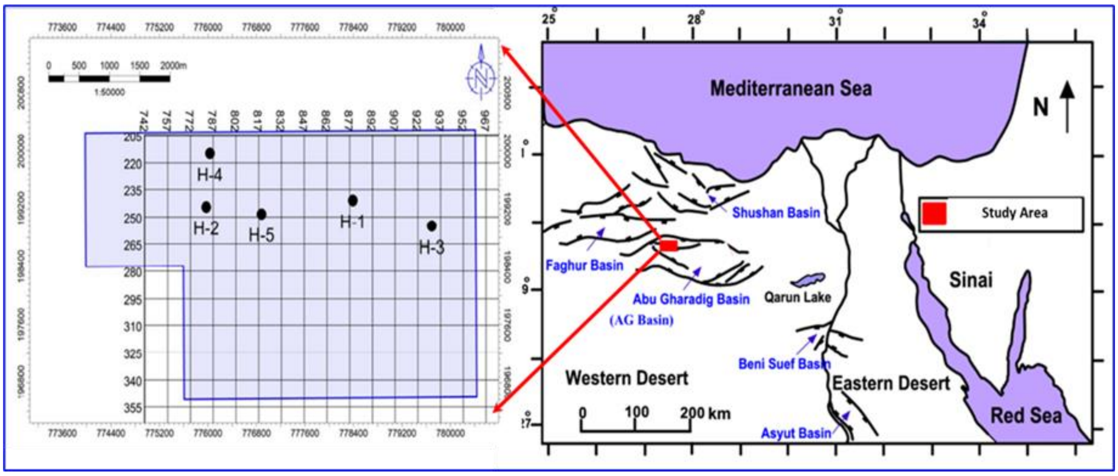

Fig. 1. The Location map of the study area.

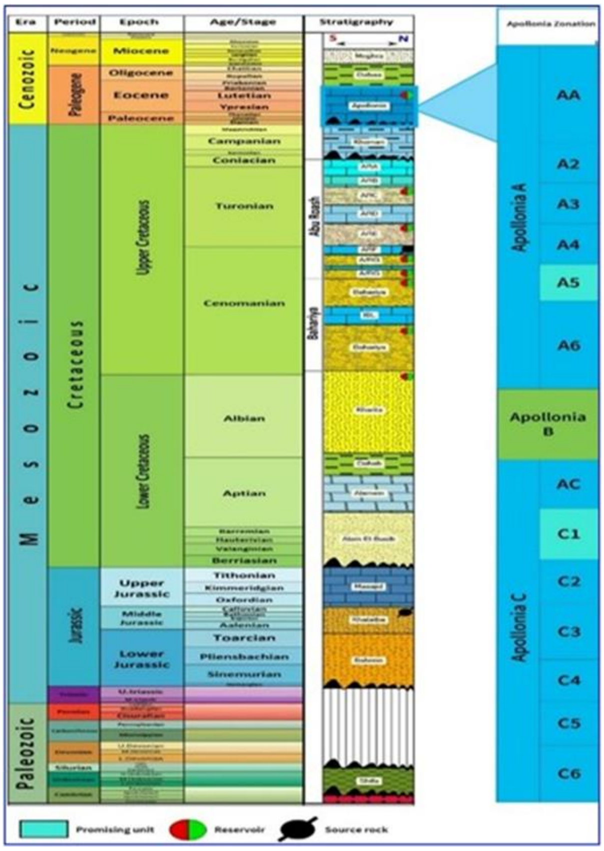

Fig. 2. The stratigraphic section of the northwestern desert contained Apollonia Formation members and their subdivision from Early Palaeocene to Middle Eocene, (modified after Rashad et al., 2024).

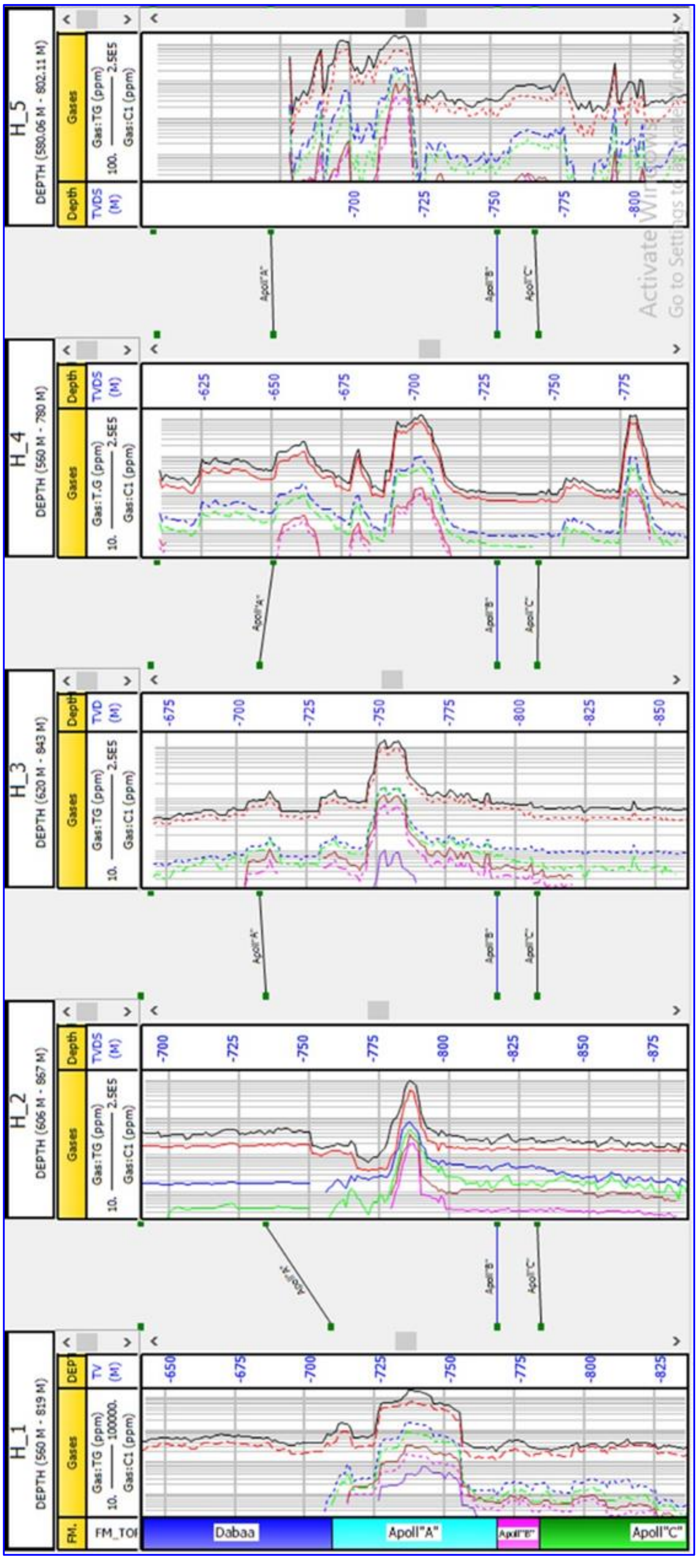

Fig. 3. Recorded high gas readings while drilling the wells of the study area.

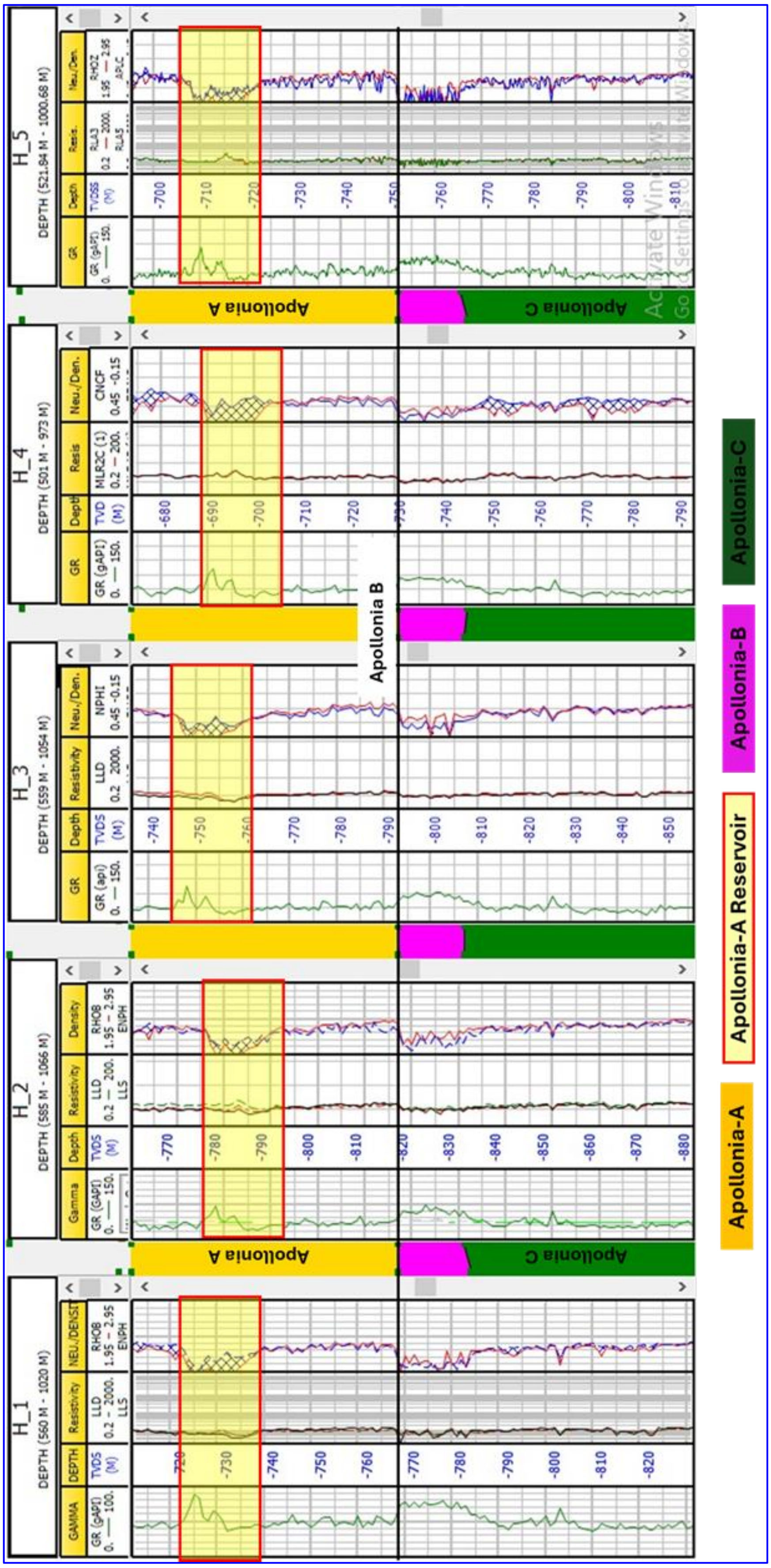

Fig. 4. The Stratigraphic correlation flattened on top Apollonia-B member across the study area.

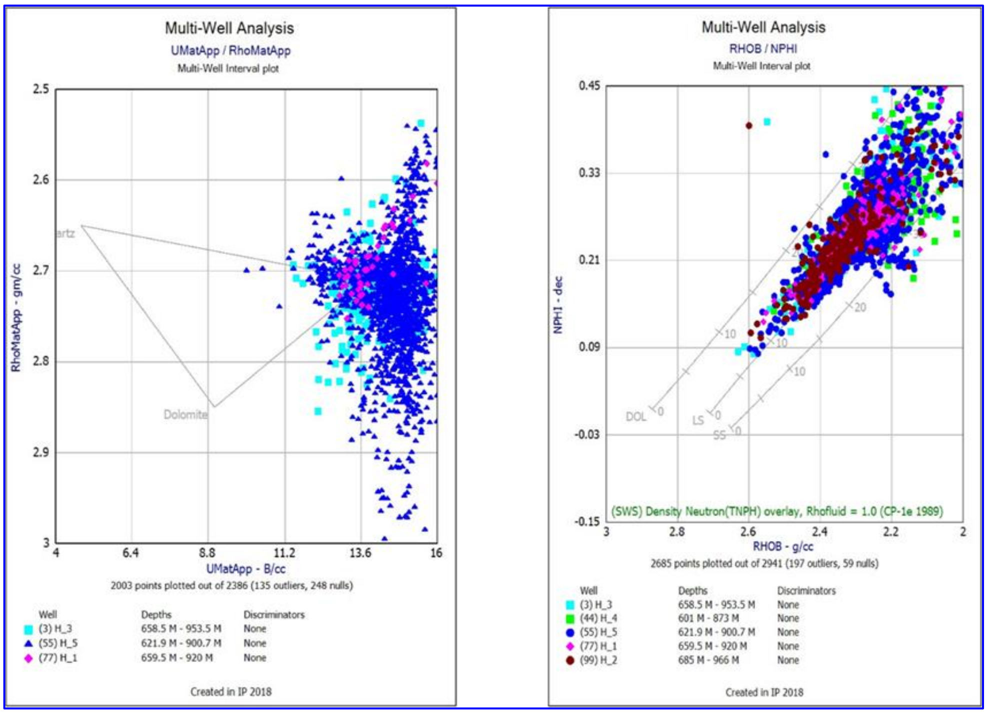

Fig. 5. Lithology determination for Apollonia-A reservoir using mullite wells 2D cross plot of Neutron-density crossplot and Umaa- ρma crossplot.

The Apollonia Formation is a thick section of limestone with subordinate shales belonging to Paleocene-middle Eocene age overlain by the Dabaa shale Formation (Oligocene-Eocene) and bottomed on unconformably surface at the Khoman Formation (Upper Cretaceous). The Apollonia Formation has been subdivided into four informal members: A; B, C and D. The Apollonia 'D' Member is the oldest and unconformably overlies the white chalky limestone of the Khoman Formation. El-Bendary et al., 2016; Elmahdy, Farag, Tarabees, & Bakr, 2018; Salah, Orr, Abdel Meguid, Crane, & Squires, 2016; Sedek & Al Mahdy, 2013; Sousa & Badri, 1996) and others studied the Apollonia Formation in detail, explaining its lithology, petrophysical characteristics, paleontological description and reservoir productivity. In the study area the Apollonia reservoir was neglected although the high gas readings with full component that was recorded across Apollonia-A reservoir that reached to 400K ppm with full components (C1-C5) (Fig.3) because of the wireline logs deep resistivity was recorded in low rang (1- 3 ohm) with clear Neutron-Density negative cross-over indicated very good porosity ,gas effect and reservoir continuity overall study area as seen in (Fig.4) that showed the stratigraphic correlation that flattened on top Apollonia-B member to figure out Apollonia-A reservoir continuity and highlight the lateral distribution of the reservoir across the study area. Lithologically identification using Neutron-Density and Umatrix-Rhomatrix 2D cross plot for Appolonia-A reservoir showed that most data located at limestone area. (Fig.5).

3. Materials and Methods

The context of this work edited data is shown in the seismic line location map, as displayed in Fig. (1). These data include 3D seismic post-stack time migration (PSTM) data covering an area of Apollonia carbonate tight reservoir, Northwest Abu El-Gharadig Basin, the seismic data in the study area ranges from First inline: 742 to inline: 1020 and from First xline 205 to Last xline: 400 (Fig.1). As well as Electrical

Logging data (quad compo) of five onshore wells (H-1, H-2, H-3, H-4 and H-5) that were drilled along the upthrown side blocks of the regional tectonic fault in the field. The Apollonia “A” pay summary shows the petrophysical characteristics of productive intervals from five wells, H1–H5, reflecting the reservoir quality and potential. Gross thickness varies between 59 and 80.1 m, while net thickness ranges from 3.5 to 8.75 m, showing that the pay zones form a limited but significant portion of the total reservoir interval. Values of the N/G ratio vary between 0.058 and 0.148, indicating localized development of effective reservoir layers. Average porosity ranges between 0.414 and 0.431, showing a moderately to well-developed pore system capable of storing and flowing fluids. The average water saturation ranges between 0.458 and 0.632, relatively high; however, as evidenced by the core analysis, this water is largely irreducible, representing water bound in the pore spaces of the carbonate matrix.

The average shale volume (0.144–0.334) represents low to moderate clay content, confirming the clean nature of the reservoir. The data pointed out that the Apollonia -A pay zones, taking into consideration core evidence, have good porosity, low shale content, and high irreducible water saturation, proving these to be potential productive gas-bearing carbonate intervals as illustrated in Table (1)

Well-to seismic ties were performed by Synthetic Seismogram Generation. In our case, the wavelet estimation is done in the time window where the match between seismic and synthetic reflectivity seems to be more reliable. A constant computation window of 200ms (between 500ms to 700ms), 120ms in length with a 50ms taper, and used Elastic-density with a central angle to that of the relative angle gathered. Then, as shown in (Fig.6).

In the study area Four key horizons, namely Bahariya, AR/G, Khoman, and the interested zone is Appolonia A which is characterized by shelf carbonate facies to pelagic chalk carbonate facies, these formations range from Cenomanian to Eocene age as displayed in (Fig.7).

The section is dominated structurally by a major fault trending through the middle to the right portion of the profile, resulting in a considerable vertical throw of the reflectors. This fault probably plays a key role in the structural configuration and may influence hydrocarbon migration and trapping. Additional minor faults are also interpreted, creating fault-bounded blocks and contributing to the local structural compartmentalization.

The mapping of subsurface layers for exploration and development typically demands a thorough comprehension of the structural framework of the field and a detailed analysis of seismic facies. This process involves interpreting and correlating existing wells nearby and connecting the areas of interest from well logs to seismic data. Subsurface mapping utilizing 3D seismic data for exploration requires a solid understanding of the basin's structural framework alongside seismic facies analysis. Conversely, mapping in developed fields integrates production outcomes with the regions of interest.

The structural framework was established after creating time and depth contour maps for the Apollonia top zone, where the marker was selected and interpolated to generate continuous horizon surfaces through the extraction of seismic attributes and various seismic attribute scanning.

The time structure contour map derived from the top of the Apollonia Formation, utilizing the 3D seismic data as shown (Fig. 7 and 8), reveals three principal fault trends: East-West, Northwest-Southeast, and Northeast-Southwest, which together create three-way dip closures distributed throughout the studied field, with the crest of the structure located at a TWT of 680 milliseconds.

The depth structural contour map produced for the top of Apollonia provides a general overview of the contemporary structures influencing the area under investigation, confirming the same fault patterns identified by the two-way time contour map, as illustrated in (Fig. 9).

Table 1. Apollonia-A petrophysical pay summar.

Well	Top (Md)	Bottom (Md)	Gross (m)	Net (m)	N/G	Avg. Φe (%)	Avg.Sw (%)	Avg.Vcl (%)
H_1	659.5	718.5	59	0.75	0.013	44.4	63.2	35.4
H_2	704.93	767	62.07	4.6	0.074	41.6	54.9	20.9
H_3	675	743	68	2.75	0.04	43.1	59.5	26.5
H_4	601	680.5	79.5	4	0.05	42.4	58	19.7
H_5	621.9	702	80.1	5.5	0.068	46	56.1	14.4

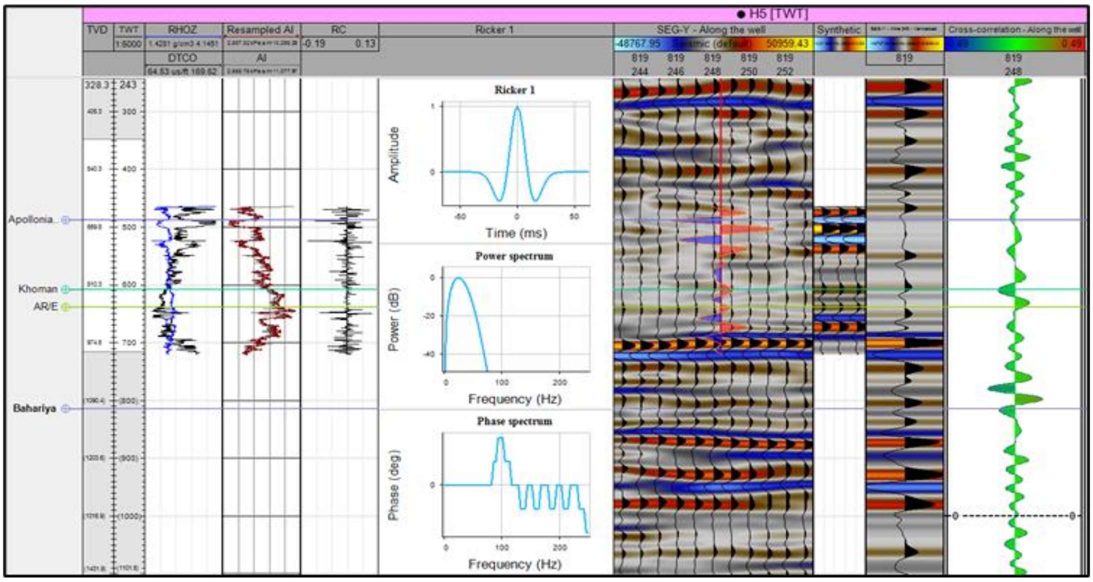

Fig. 6. Synthetic seismogram constructed for well H5 using statistical-type wavelet.

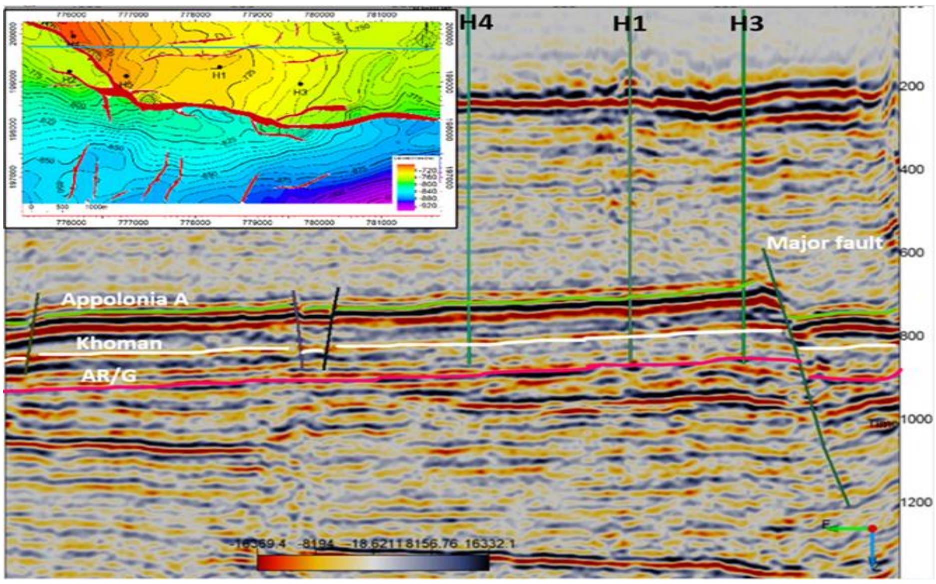

Fig. 7. E-W Seismic Section Shows the main normal fault and three wells on the upthrown side of the study area.

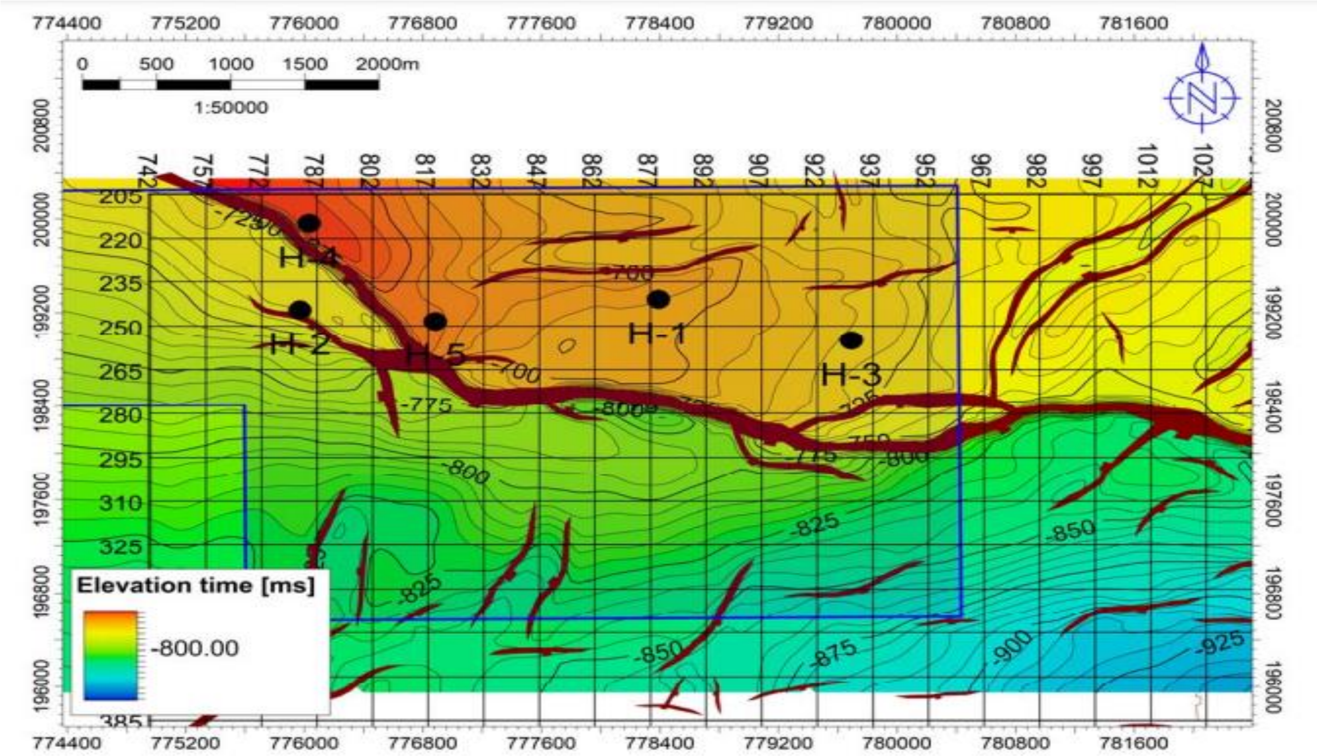

Fig. 8. Regional Time structure contour map for top Apollonia-A in the study area.

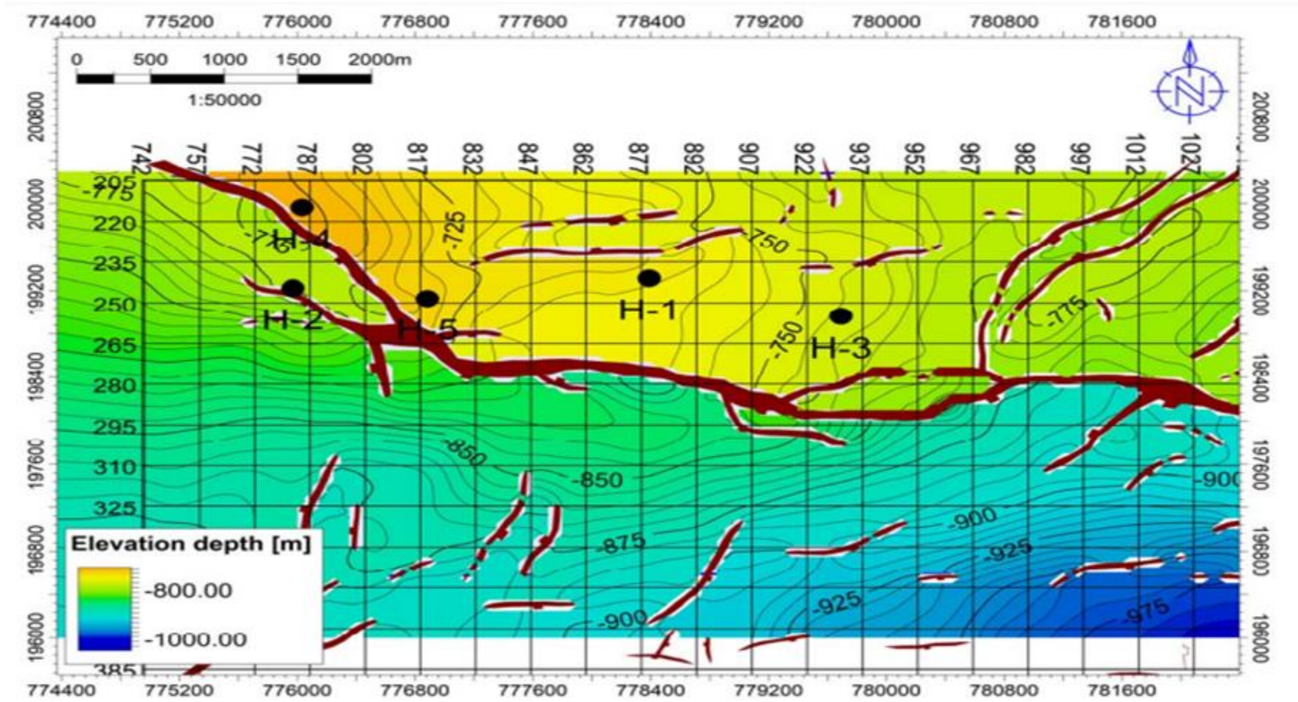

Fig. 9. Depth structure contour map for top Apollonia-A in the study area.

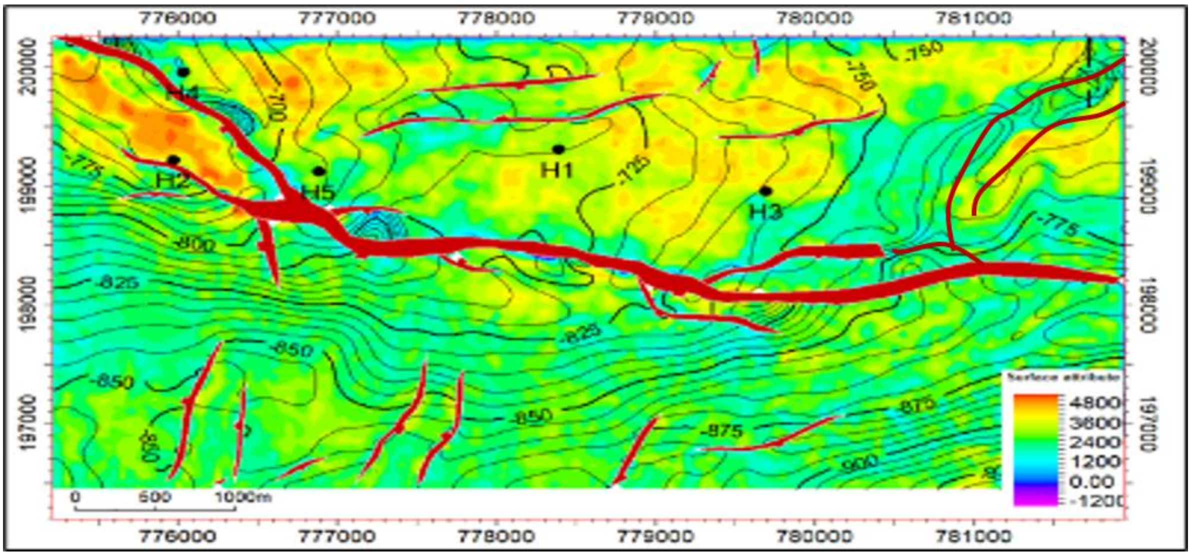

Fig. 10. 2D Map View of Interpreting Top Appolonia-A with RMS Surface Amplitude attribute.

The combination between depth contour maps the RMS amplitude to reveal structural trends, highlighting higher amplitudes in certain parts of the structures depicted in hot colors (yellow to red) in (Fig. 10). This could indicate fluid or stratigraphic variations, such as gas accumulations. In this study, we calculated the variance, similarity, RMS amplitude, and energy seismic attributes of the 3D seismic volume to map sand bodies and discontinuities within the study area, respectively. The characterization of reservoirs using RMS amplitude and energy attributes is essential, as these high amplitudes indicate lithological variations laterally and the likelihood of hydrocarbon presence (Gridley and Partyka 1997; Partyka et al. 1999). Conversely, analyzing both variance and similarity attributes of surfaces is vital for mitigating regional dip effects and highlighting small-scale features that may be related to primary depositional characteristics or minor faults (Chopra and Marfurt 2006).

Spectral decomposition of seismic data refers to the variations in seismic amplitudes over space and time, transforming them into spectral amplitudes as they relate to frequency and phase (Gridley and Partyka 1997; Partyka et al. 1999). This approach has been utilized to define and enhance imaging of facies and depositional environments (Peyton et al. 1998). In this study, the Fast Fourier Transform (FFT) is employed on comprehensive, high-resolution 3D seismic data to identify the structural framework and reservoir lithology of the Apollonia formation. To accomplish this, three distinct FFT frequencies were applied concerning faults and perspectives on reservoir lithology. These three frequencies were subsequently merged to obtain the FFT response in relation to various conventional seismic attributes.

4. Results and Discussions

4.1 Curvature seismic attribute

The variance attributes measure the similarity between adjacent seismic traces, making it an effective tool for imaging major fault zones, fractures, unconformities, and sequence boundaries (Pigott et al., 2013). As shown in (Fig.11), variance time slices at 1744 ms and 1770 ms were applied to the 3D seismic data to enhance discontinuities within the highly faulted Apollonia A reservoir. The numerous linear features revealed by the attribute confirm the reservoir's complex faulting. The results exhibited by applying variance seismic attributes have a similarity, to the results exhibited by applying the similarity seismic attribute (Fig.12) on the same dataset. However, there are some differences in the faults visualization that should be considered. variance attributes exhibit high faults density with a small horizontal spacing between these faults of. This fault trace is more than three times the traces that appeared by the similarity attribute. This refers to the probability of the presence of many faults on the variance depth slice that could not appear on the similarity time slice.

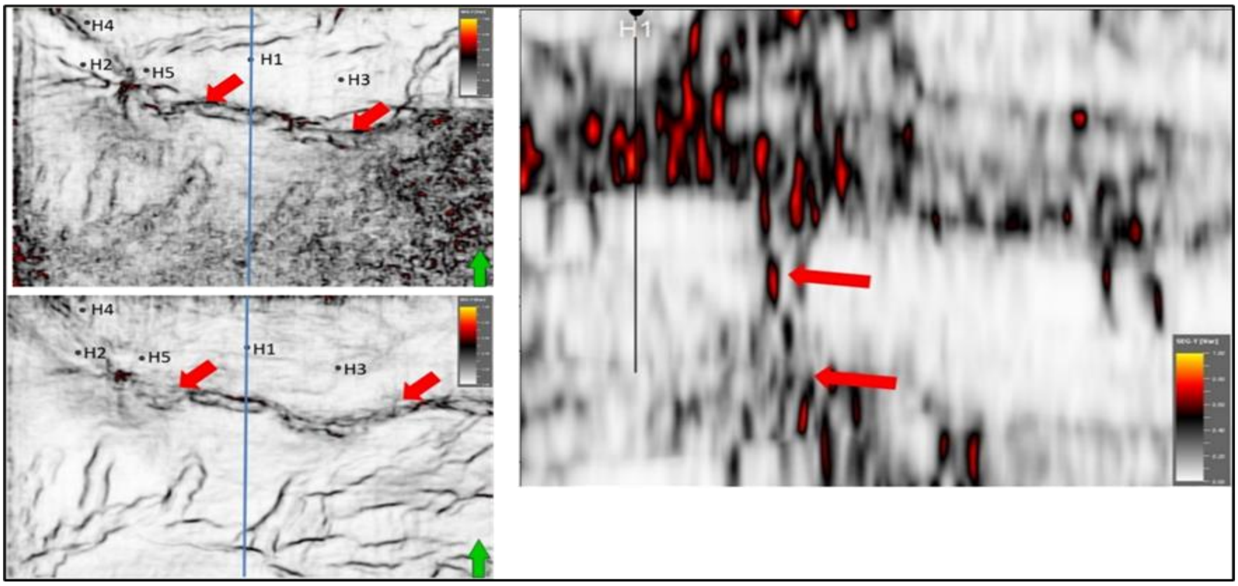

Fig. 11. Variance time slices at 1744 and 1770 ms approximately along the Apollonia A layer, showing the main faults (indicated by red arrow) affecting the Apollonia A Reservoir along the study area in Abu El-Gharadig Basin.

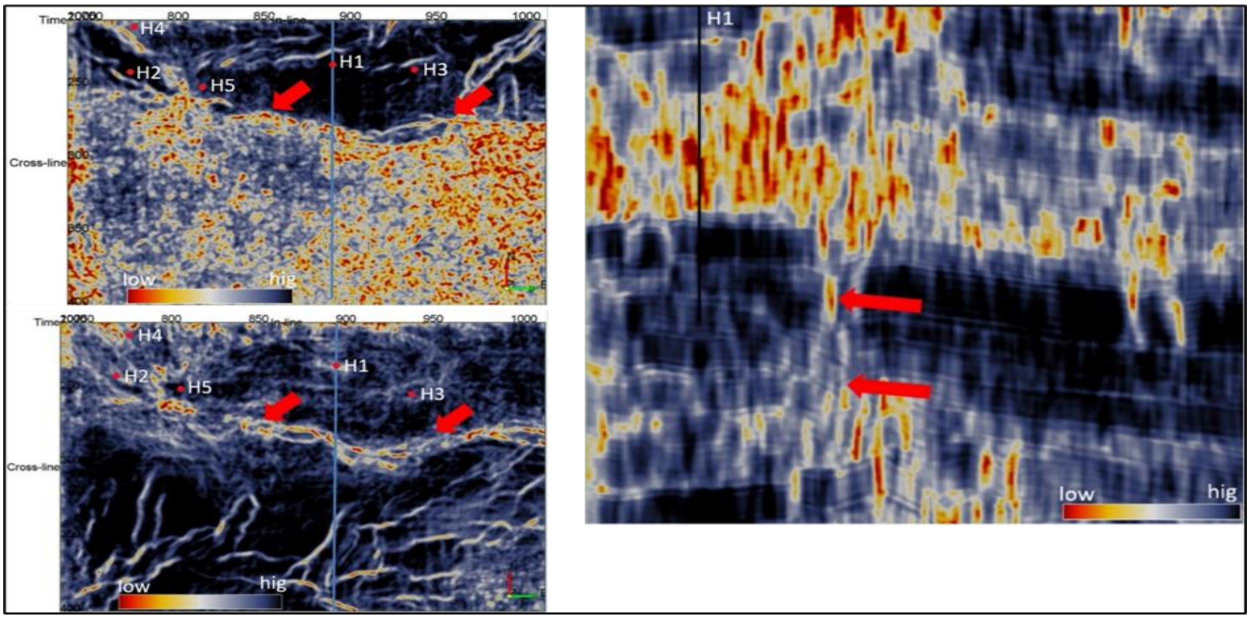

Fig. 12. Similarity attribute depth slices at 1744 and 1770 ms approximately along the Apollonia A5 layer confirmed the main faults (indicated by red arrow) affecting the Apollonia Formation along the study area in Abu El-Gharadig.

4.2 Energy and RMS attributes

This seismic characteristic is regarded as one of the key indicators of oil presence and can be described as: the squared sum of the selected values within a specified time gate divided by the number of samples chosen in that same gate. The energy attribute serves as an effective means for estimating reflectivity in the defined time gate. A greater Energy signature corresponds to a greater Amplitude. The energy attribute is determined as the mean squared amplitude in a specified time gate, offering a measurement of reflectivity. Increased energy values are directly associated with increased amplitudes. This attribute aids in enhancing lateral variations in seismic events, proving beneficial for identifying features such as chimneys. Additionally, it assists in characterizing acoustic rock properties and bed thickness. According to Tingdahl, 2003, the energy attribute is defined as:

$$E = \sum_{\tau=t1}^{t2} u(x, y, t+\tau)\,2 \qquad (1)$$

Here, t1 and t2 represent the start and end times of the energy calculation window.

Fig.13 displays the energy attribute map that demonstrates the spatial distribution of reflection strength and emphasizes the contrasts in acoustic impedance within the Apollonia carbonate reservoir zone. The high-energy regions, represented in red and yellow, primarily occur between 250 and 300 ms, signifying areas with a favorable seismic response. These amplitude peaks are interpreted as widespread accumulations of carbonates with significant impedance contrast between the porous, hydrocarbon-rich facies and the adjacent compacted or dense carbonates. The presence of elevated energy levels near wells H1, H3, and H5 indicates potential reservoir formations linked to reefal or platform-margin carbonates, where porosity may be improved through diagenetic processes such as dissolution or fracturing. Conversely, the adjacent blue to green regions indicate low-energy reactions that are similar to dense, non-porous layers of limestone or shale, which serve as non-reservoir or sealing formations. Variations in lateral facies energy levels suggest diversity in the carbonate accumulation, potentially resulting in differences in porosity and fluid saturation. Overall, the map effectively outlines the shape and extent of the productive carbonate formation, with high-energy anomalies indicating the most promising reservoir areas for hydrocarbon accumulation. Seismic or gas chimney features evident in the seismic data appear as chaotic, low-amplitude, and low-energy characteristics. The chimneys are characterized as low amplitude and low energy disturbed events. This type of seismic attribute is the most prevalent, and amplitude is frequently associated with porosity and liquid saturation. A trough corresponds to a negative amplitude, while a peak represents a positive amplitude in the seismic trace. The larger the peak or trough, the more significant the positive or negative amplitude values. The upthrown section of the study area is primarily depicted by a high amplitude value (indicated in yellow to red), classified as hot colors, while the downthrown section is illustrated by a low amplitude value (shown in greenish blue).

This amplitude map of seismic measurements, obtained from the Apollonia carbonate reservoir, highlights a prominent high-amplitude anomaly (the red/yellow anomaly) indicative of a significant geological sweet spot. In carbonate formations, the bright and intense signal not only indicates the presence of liquid but is also a result of significantly enhanced secondary porosity, often due to strong diagenetic processes such as karstification (dissolution that creates vugs and caves), whereby the existence of gas further decreases acoustic impedance, enhancing the response. The eroded, irregular edge of the anomaly contrasted against the low-amplitude blue background suggests that the quality reservoir rock is closely bordered by a transition zone of depositional facies. Wells H1 and H3 are strategically positioned to take advantage of this sweet spot, with expectations of high porosity and flow rates, while well H5 is situated to explore the lateral extents and potential hydrocarbon-water contact. In contrast, wells H2 and H4, located within the low-amplitude blue area, will intersect the dense, low-porosity rock typical of many carbonate platforms and act as non-productive reference points to validate the quality reservoir boundaries as illustrated in (Fig.15).

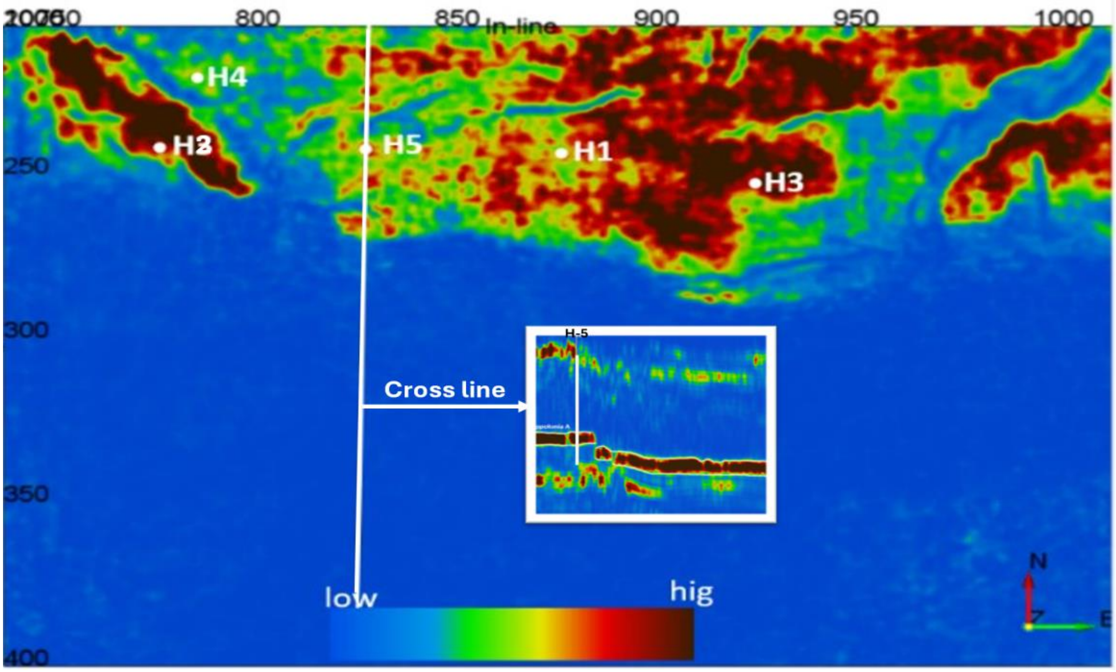

Fig. 13. The energy amplitude time slice at 1744 ms shows the amplitude distribution along the Appolonia A, and seismic section passing through the H5 well.

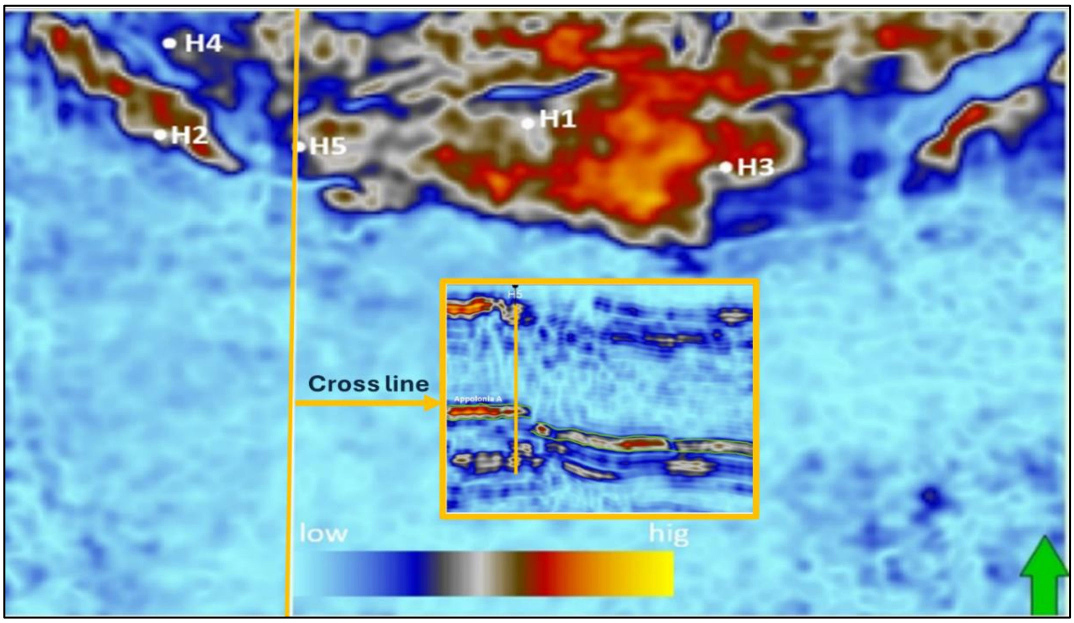

Fig. 14. The RMS amplitude time slice at 1744 ms shows the amplitude distribution along the Appolonia A, and seismic section passing through the H5 well.

4.3 Spectral Decomposition

The spectral decomposition workflows in this study focused on processing Discrete Fourier Transform (DFT) around a very smooth seismic horizon interpretation, transforming the amplitude or phase data into the frequency domain. The dominant frequency of seismic data, approximately 25 Hz, was determined prior to running spectral decomposition (Fig.15). It is important to note that the tuning frequency of specific intervals may differ from this overall dominant frequency. Spectral decomposition was applied to analyses the amplitude distribution across different frequency bands. A Red-Green-Blue (RGB) blending technique was then used to combine three selected frequency volumes, allowing the frequency response of the reservoir to be clearly identified by its unique color signature.

Six single-frequency windows, ranging from 5 Hz to 50 Hz, were generated for analysis (Fig.16). Two RGB blending trials were conducted to optimize the results. The first trial combined 10 Hz (assigned to red), 25 Hz (the dataset's dominant frequency, assigned to green), and 50 Hz (the highest frequency, assigned to blue). The second trial used 5 Hz (red), 20 Hz (green, the dominant frequency), and 40 Hz (blue), as shown in (Fig.16).

The final RGB blend is presented in (Fig 17), which reveals a correlation between seismic attributes and frequency response. Wells H1 and H4 coincide with high RMS amplitude and energy values, which correspond to low-frequency zones on the RGB slice. In contrast, while wells H-2, H-3, and H-5 also exhibit high amplitude and energy, they are associated with a mid-frequency response on the RGB blend.

Notably, parts of the upthrown side of the study area appear white in the RGB blend, indicating a balanced mix of all frequency ranges. This signature is interpreted to represent the thickest parts of the reservoir and suggests hydrocarbon presence. These prospective areas, indicated by red circles in (Fig.18), are therefore considered promising targets.

While at H-5, H-3, and H-2 well the RMS amplitude and energy attributes appear as high, but on the RGB blended slice indicated as middle frequency, in addition, some parts of the upthrown side of the study area appear in white color which means they contain all frequency ranges; this corresponds to the thickest parts of the reservoir and its indication on the presence of hydrocarbon so these parts indicated by red circle considered a good prospect. (Fig.18) clearly shows the study area affected by a major NW-SE fault classifying into two main blocks Also, this result can be observed at different frequency values where the different characteristic becomes more notable, and a more comprehensive results can be shown at the peak frequency of the seismic data. As it can be noted that the main faults are become more tuned, and the minor faults and the small lineaments are also getting tuned with higher the frequency value more comprehensive results can be shown at the peak frequency of the seismic.

The potential zones illustrated in (Fig.18) can be listed in Table .2 and described as follows:

- High Potential

Zone 5 (Rank 1): This is the most robust reservoir. The combination of High, laterally continuous amplitude and Strong, focused energy suggests a high-quality, continuous reservoir unit. Well-log data confirm excellent porosity and hydrocarbon saturation (Phie = 41.6%, Gas saturation = 44%), and this area should be the primary drilling target. This zone encompasses the area within the anomaly of the prospective zones and includes the confirmed gas location H-2

Zone 1 (Rank 2): While not as robust as Zone 5, it possesses a Moderate amplitude with fair lateral continuity and Strong, concentrated energy, coupled with the desirable Yellow-Green-White mix (broadband) spectral response. Although there are No E-Logs to confirm, the seismic attributes strongly indicate that this is a good reservoir.

- Moderate Potential

Zone 4 (Rank 3): This zone has low and weak lateral continuity but shows Moderate energy with the presence of localized bright spots. Surprisingly, the well-log data constructed in H-5 well shows the highest porosity of Phie = 46%, Gas saturation= 44%, indicating that the reservoir is likely to be patchy or thin but, where present, holds excellent quality. It represents a potential target but with higher drilling risk due to poor continuity. The well logs override the spatial constraint, confirming very good flow potential. The interpretation is that Zone-4 solves a highly localized, high-quality feature (presumably a tight fracture) that is productive despite being extremely small.

Zone 2 (Rank 4): Even though the High with localize bright spot amplitude, the attributes overall are less convincing than Zone 1. The patchy high frequency in the spectral decomposition suggests heterogeneity. It has a confirmed reservoir but with slightly lower porosity of Φe = 43%. The effective flow potential here is considerably weaker than in Zones 4, 5, and 1, per the logs. The type of area one has in mind here is a gigantic volume of high-porosity, gas-saturated rock with very poor connectivity. Development in this place will require the most vigorous and costly hydraulic fracturing program to achieve commercial flow rates and should be secondary to successful development of the more productive higher-flow zones.

- Low Potential

Zone 3-Rank 5: This is a low-priority zone. The attributes are unremarkable, characterized by Moderate-High amplitude with variable continuity and Moderate, evenly distributed energy. The dominance of the Green ≈ 25 Hz mid frequency and confirmation by No E-Logs renders it the riskiest and least attractive target based purely on seismic data.

Even though it occupies a reasonable space among the potential zones, it has no certain gas spot and is defined from the well logs to have the poorest overall reservoir quality and flow capacity. This is the least promising and could be utilized only for development when all the higher-ranked zones are in full use.

The indications from the data, therefore, unequivocally call for a tiered exploration strategy: Zone 5 and Zone 1 as priority areas, followed by focused appraisal of Zone 4 and Zone 2.

Table 2. Summary of Reservoir Quality ranking derived from seismic attributes and well data.

Zone	RMS Amplitude	Energy Attribute	Spectral Decomposition (RGB 5-25-65 Hz)	Reservoir Quality	Rank
1	Moderate with fair lateral continuity	Strong, concentrated indicating clear impedance	Yellow-Green-White mix (25 Hz increasing broadband overlap to 65 Hz) strong internal contrast	No E-Logs	2
2	High with localize bright spot	Strong-Moderate	Green-Yellow-White localize broadband overlap -patchy high frequency	H-3 well E-logs showed Φe= 43% and Gas saturation 40%	4
3	Moderate-High with variable continuity	Moderate, evenly distributed	Green ≈ (25 Hz) mid frequency response with localize bright patches	No E-Logs	5
4	Low and weak lateral continuity	Moderate	Green ≈ (25 Hz) mid frequency character, moderate continuity and localize bright spots	H-5 well E-logs showed Φe= 46% and Gas saturation 44%	3
5	High, laterally continuous amplitude	Strong, focused energy suggesting robust reflection strength and reservoir continuity	Broadband overlaps white /yellow -white central bright zone (5+25+65 Hz) very strong broadband energy and continuity	H-2 well E-logs showed Φe= 41.6% and Gas saturation 44%	1

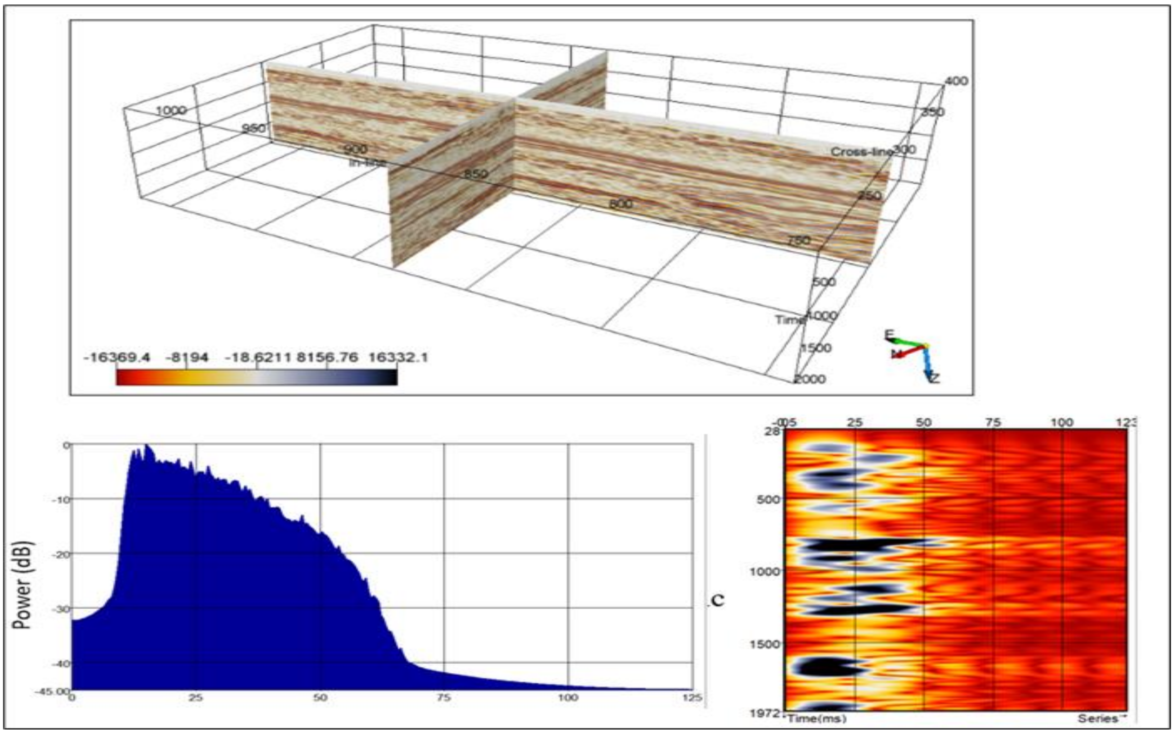

Fig. 15. Amplitude Spectrum for the full seismic data within the reservoir interval.

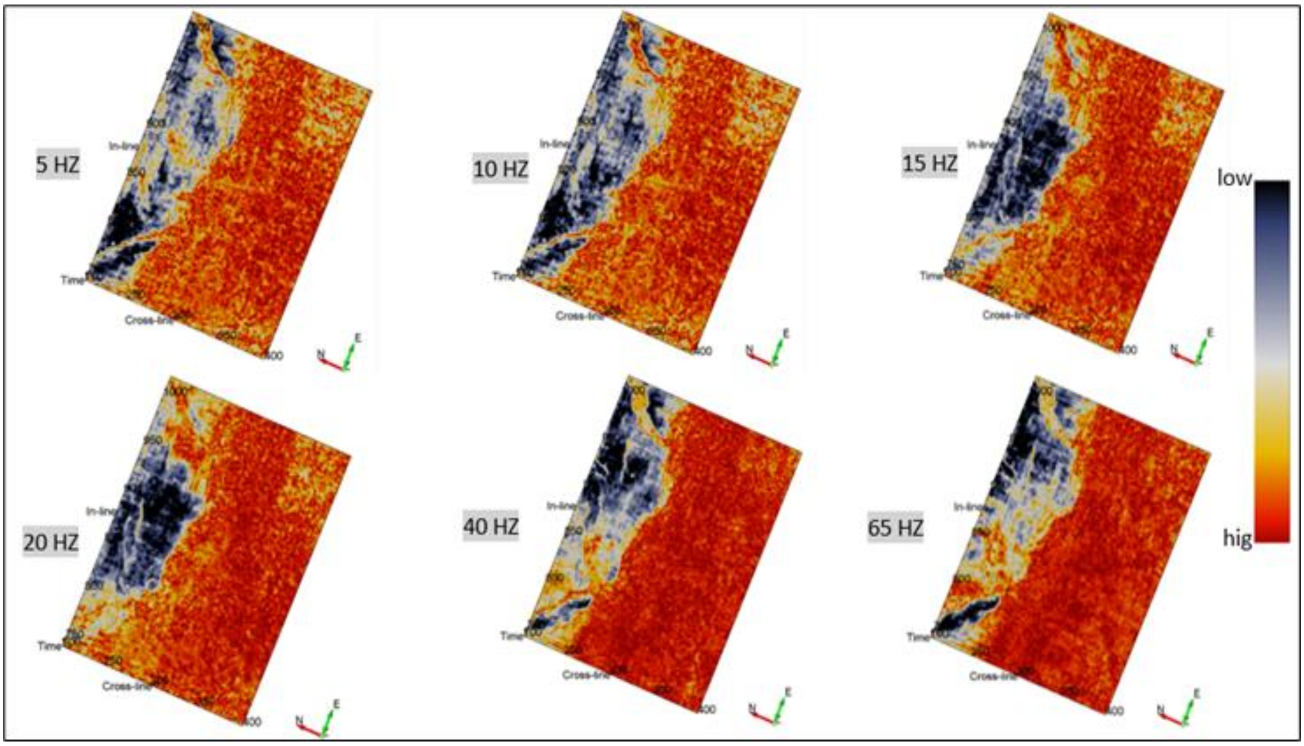

Fig. 16. Six basic frequency ranges used for red, green, and blue color blending.

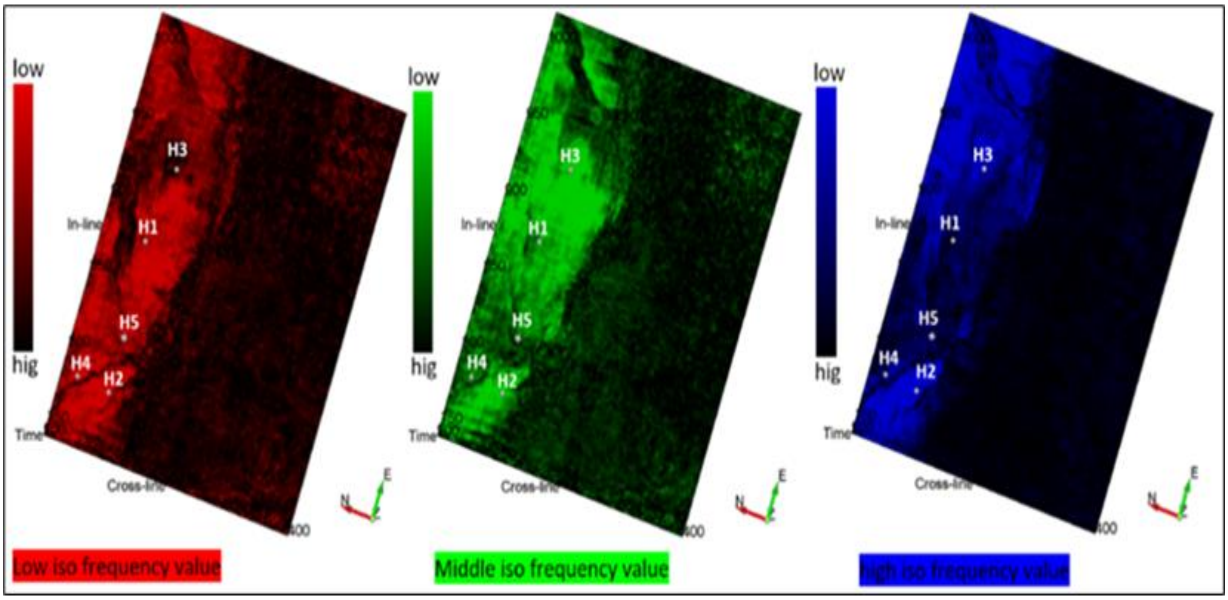

Fig. 17. The amplitude variation of the interesting zone on different common frequency sections (above) and red, green, and blue values calculated by three basic frequencies the three frequency ranges are: 5 Hz in Red color, 25 Hz in Green color, and 50 Hz in Blue color.

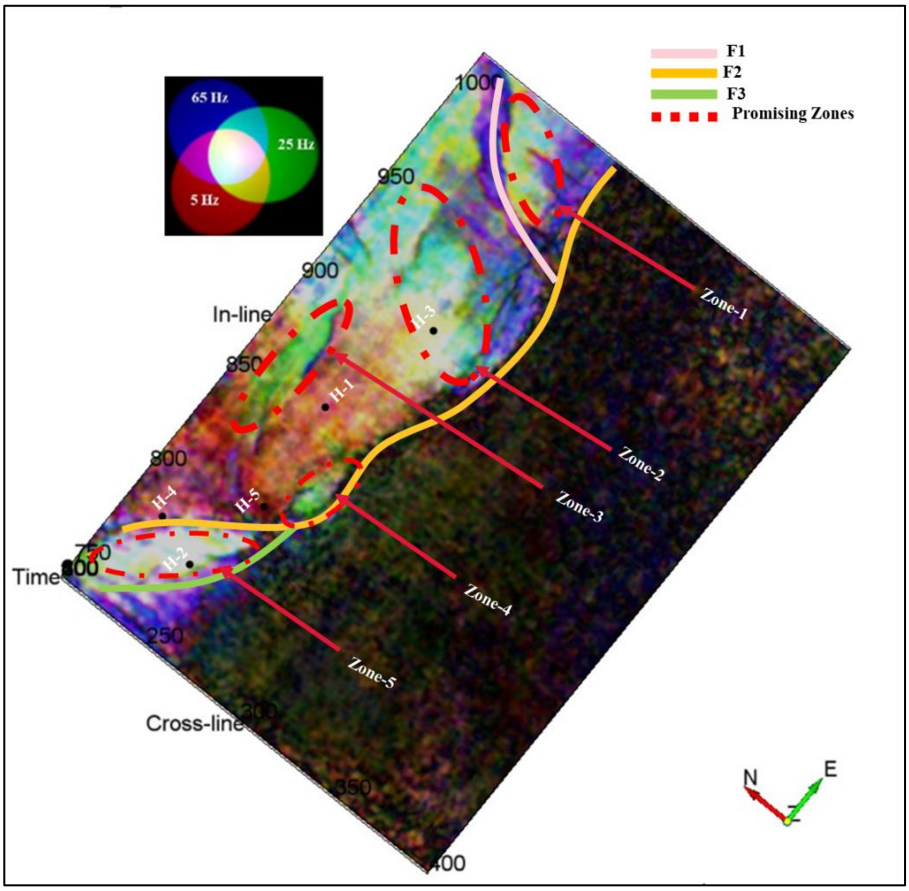

Fig. 18. The result color blended frequency volume over the Appolonia A.

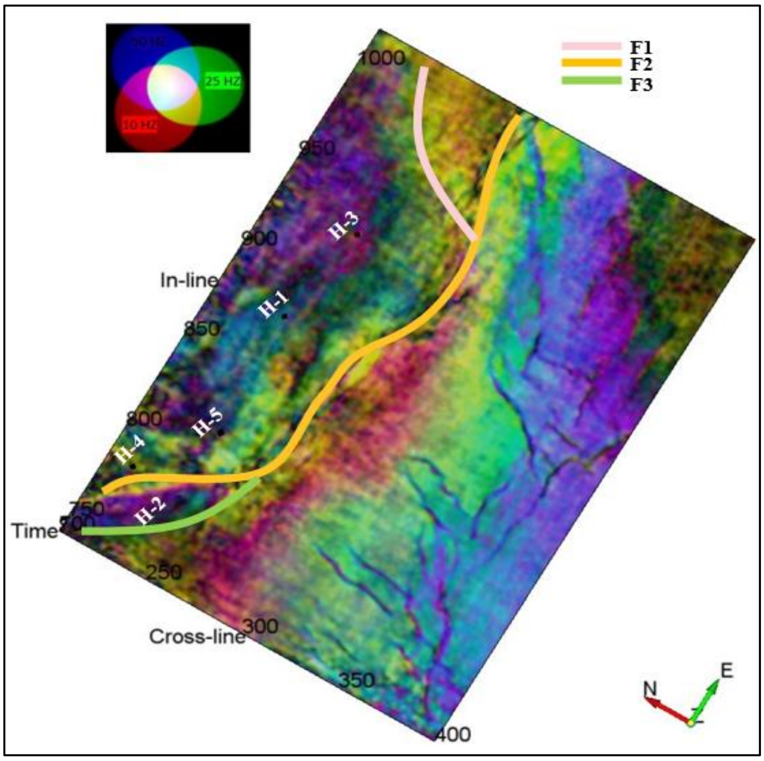

Fig. 19. Color blended frequency map showing clearly the structures affected of the downthrown side of the study area.

5. Conclusions

The structural configuration identified on top of the Apollonia reservoir using 3D seismic data reveals three predominant fault trends: E-W, NW-SE, and NE-SW, which together create a three-way dip closure.

Energy and RMS attributes effectively highlight high-reflection zones that correlate with porous and gas-bearing carbonate structures. The lateral continuity and significant amplitude responses of the anomalies indicate well-established reservoir facies with notable impedance contrasts, underscoring the effectiveness of energy attributes in recognizing and mapping productive carbonate regions.

The curvature and similarity attributes utilized in this analysis are valuable for visualizing the faults impacting the reservoir and clearly depict the main NW-SE fault that separates the area into an upthrown side and downthrown side, these methods are inadequate for detecting potential reservoir lithologies within the area of interest.

The use of Fourier transformations of spectral decomposition is essential for accurately visualizing faults throughout the reservoir, offering promising indicators for future hydrocarbon exploration and development. The study concluded that the implementation of spectral analysis and 3D imaging enabled the identification of multiple future gas prospects within the Apollonia Formation in the examined areas, which are illustrated and ranked from high to low as follows: Zone-5, Zone-1, Zone-4, Zone-2, and the lowest, Zone-3.

Ethics approval and consent to participate:

This article does not contain any studies with human participants or animals performed by any of the authors.

Consent for publication: All authors declare their consent for publication.

Funding

The authors did not receive support from any organization for the submitted work; the work depends on their own expenses.

Conflicts of Interest: The author declares no conflict of interest.

Contribution of Authors: All authors shared in writing, editing and revising the MS and agree to its publication.

Acknowledgement:

providing the data to conduct and implement the study, The authors sincerely thank the Geology Department, Faculty of Science, Al Azhar University for technical assistance and constructive discussions.

References

Alrefaee, H.A., Gosh, S., Abdel-Fattah, M.I., (2018). 3D seismic characterization of the polygonal fault systems and its impact on fluid flow migration: an example from the Northern Carnarvon Basin, Australia. J. Petrol. Sci. Eng. 167, 120–130. https://doi. org/10.1016/j.petrol.2018.04.009.

Antonellini, M., Cilona, A., Tondi, E., Zambrano, M., Agosta, F., (2014). Fluid flow numerical experiments of faulted porous carbonates, Northwest Sicily (Italy). Mar. Petrol. Geol. 55, 186–201. https://doi.org/10.1016/j.marpetgeo.2013.12.003.

Bhattacharya, S., Verma, S., (2019). Application of volumetric seismic attributes for complex fault network characterization on the North Slope, Alaska. J. Nat. Gas Sci. Eng. 65, 56–67. https://doi.org/10.1016/j.jngse.2019.02.002.

Cerepi, A., Barde, J.P., Labat, N., (2003). High-resolution characterization and integrated study of a reservoir formation: the danian carbonate platform in the Aquitaine Basin (France). Mar. Petrol. Geol. 20 (10), 1161–1183. https://doi.org/10.1016/j. marpetgeo.2003.09.005.

Childs, C., Walsh, J.J., Watterson, J., (1990). A method for estimating the density of fault displacements below the limits of seismic resolution in reservoir formations. In: Buller, A.T., Berg, E., Hjelmeland, O., Kleppe, J., Torsæter, O., Aasen, J.O. (Eds.), North Sea Oil and Gas Reservoirs II. Graham and Trotman, London, pp. 193–203. https://doi.org/10.1007/978-94-009-0791-1_26.

Chopra S, Marfurt K (2006) Seismic attributes a promising aid for geologic prediction. CSEG Rec. special edition: 110-121

EGPC Egyptian General Petroleum Corporation, (1992). Western Desert, oil and gas fields (A comprehensive overview). In: EGPC 11th Petroleum Exploration and Production Conference, p. 431. Cairo.

El- Bendary, A., Faraga, Y., Abo-Elabas, S., Magde, M., Moukhtar, A., Ramadan, H., (2016). Critical Success Factors Identification to develop unconventional high porosity low permeability shallow limestone reservoir of Apollonia formation, western desert Egypt. In: Abu Dhabi International Petroleum Exhibition and Conference, United Arab of Emirates. Society of Petroleum Engineers doi.org/10.2118/183471-MS.

El Gazzar, A.M., Moustafa, A.R., Bentham, P., (2016). Structural evolution of the Abu Gharadig field area, northern Western Desert, Egypt. J. Afr. Earth Sci. 124, 340354.https://doi.org/10.1016/j.jafrearsci.2016.09.027.

Elmahdy, M., Farag, A.E., Tarabees, E., Bakr, A., (2018). Pore pressure prediction in an unconventional carbonate reservoir. In: Society of Petroleum Engineers Kingdom of Saudi Arabia, Annual Technical Symposium and Exhibition. https://doi.org/ 10.2118/194224-MS. Dammam.

El-Gawad, Abd, et al. "Reservoir characterization of the upper Abu Roash “G” sandstone in west of Nile area, western desert, Egypt." Al-Azhar Bulletin of Science 32.2-D (2021): 23-31.

Bekhiet, M. H., et al. "Subsurface Structural and Petrophysical Study on Karama Field, East Bahariya Concession, Western Desert, Egypt." Al-Azhar Bulletin of Science 22.2-D (2011): 61-79.

Fahmy WA, Matteucci G, Butters D, Zhang J, Castagna J (2005). Successful application of spectral decomposition technology toward drilling of a key offshore development well. 75th Annual International Meeting, Society of Exploration Geophysicists Expanded Abstracts: 262-264

Gridley J, Partyka G (1997). Processing and interpretational aspects of spectral decomposition. SEG Expanded Abstracts 16:1055–1058

. Hantar, G., (1990). Northwestern Desert. In: Said, R. (Ed.), The Geology of Egypt. AA Balkema, Rotterdam, Netherlands, pp. 293–319.

Hunt, L., Reynolds, S., Brown, T., Hadley, S., Downton, J., Chopra, S., (2010). Quantitative estimate of fracture density variations in the Nordegg with azimuthal AVO and curvature: a case study. Lead. Edge 29 (9), 1122–1137.

Hussien, M. M., Abdel-Hafeez, T. H., Fathy, M. M., & El-Ghamry, M. N. (2021). Petroleum system of Gindi Basin and Mubarak Sub-Basin, Qarun Concession, Western Desert, Egypt." Al-Azhar Bulletin of Science 32.2-D 33-48.

Jahan, I., Castagna, J., Murphy, M., Kayali, M.A., (2017). Fault detection using principal component analysis of seismic attributes in the Bakken Formation, Williston Basin, North Dakota, USA. Interpretation 5 (3), 361–372. https://doi.org/10.1190/INT- 2016-0209.1.

Lohr, T., Krawczyk, C.M., Tanner, D.C., Samiee, R., Endres, H., Thierer, P.O., Oncken, O., Trappe, H., Bachmann, R., Kukla, P.A., (2008). Prediction of sub seismic faults and fractures: integration of three-dimensional seismic data, three-dimensional retro deformation, and well data on an example of deformation around an inverted fault. AAPG (Am. Assoc. Pet. Geol.) Bull. 92, 473–485.

Marzouk, A.M., (2002). Biostratigraphical and ecological significance of calcareous nannofossil assemblages from subsurface (Paleogene) sections in the Abu Gharadig field, Western Desert, Egypt, 9th INA conference, Parma, Abstracts and program J. Nannoplankton Res. 24 (2), 136–eoa.

Maerten, L., Maerten, F., (2006). Chronologic modeling of faulted and fractured reservoirs using geomechanically based restoration: technique and industry applications. AAPG (Am. Assoc. Pet. Geol.) Bull. 92, 1201–1226. https://doi.org/10.1306/ 02240605116.

Meshref, W., (1990). Tectonic framework of global tectonics. In: Said, R. (Ed.), The Geology of Egypt. AA Balkema, Rotterdam, pp. 439–449.

Partyka G, Gridley J, Lopez J (1999) Interpretational applications of spectral decomposition in reservoir characterization. Lead Edge 18:353–360

Pearce, M.A., Jones, R.R., Smith, S.A.F., McCaffrey, K.J.W., (2011). Quantification of fold curvature and fracturing using terrestrial laser scanning. AAPG (Am. Assoc. Pet. Geol.) Bull. 95, 771–794.

Peyton L, Bottjer R, Partyka G (1998) Interpretation of incised valleys using new 3-D seismic techniques: a case history using spectral decomposition and coherency. Lead Edge 17:1294–1298

Salah, M., O, D., Abdel Meguid, A., Crane, B., Squires, S., (2016). Multistage horizontal hydraulic fracture optimization through an integrated design and workflow in Apollonia tight chalk, Egypt from the laboratory to the field. Society of Petroleum Engineers. In: Abu Dhabi International Petroleum Exhibition and Conference, United Arab of Emirates. https://doi.org/10.2118/183068-MS.

Sedek, M., Al Mahdy, O., (2013). Inverted basin analysis and geological modeling, Razzak oil field, Western Desert, Egypt. Arab. J. Geosci. 6 (7), 2261–2283. https://doi:10 .1007/s12517-011-0511-4.

Shamah, K., Andrawis, S., Allam, A., El Maradny, M., (1993). Biostratigraphy of upper cretaceous-lower Tertiary boundary from E. Faghur-1, N. Ghazalat-1 and G.P.J.-2 (Abu Sennan) wells in northwestern Desert. Ann. Geol. Surv. Egypt 19, 223–243.

Verma, S., Mutlu, O., Ha, T., Bailey, W., Marfurt, K.J., (2015). Calibration of attribute anomalies through prestack seismic modeling. Interpretation 3 (4), 55–70. https:// doi.org/10.1190/INT-2015-0072.1.

Walsh, J., Watterson, J., Health, A., Childs, C., (1998). Representation and scaling of faults in fluid flow models. Petrol.Geosci.4,241–251. https://doi.org/10.1144/petgeo.4.3.241.

تكامل السمات الزلزالية والتحلل الطيفي لتوصيف الخزانات تكوين أبولونيا شمال غرب حوض أبو الغراديق، مصر

محمود شعير[1]، ومحمود يسري زين الدين[1]، وبدر عباس خليل[2]

[1] قسم الجيولوجيا، كلية العلوم، جامعة الأزهر، القاهرة، مصر

[2] شركة اتش بي اس للبترول 12 شارع النادي الجديد المعادي الجديدة، القاهرة، مصر

ظل خزان أبولونيا الكربوني غير التقليدي مهمل في منطقة الدراسة لسنوات حيث لم يكن الهدف الأول في الإنتاج رغم انه تم تسجيل قراءات عالية جدا للغازات المصاحبة لعمليات الحفر، ولكن عند التسجيل الكهربائي للخزان يظهر نتائج سلبية يتميز خزاننا من الناحية الصخرية بمسامية عالية تتراوح بين 12 و 45 % بمتوسط 32% ونسبة عالية من تشبع الماء ونفاذية منخفضة للغاية بحد أقصى 1.5مللي دارسي والتي تحتاج إلى المزيد من عمليات التحفيز (التحميض والتكسير الهيدروليكي) و مؤخرا تم التركيز عليه وإعادة تقييمه بوجهة نظر اخري لمعرفة الاحتياطي ومدي الفعالية العملياتية والاقتصادية من خطط التنمية.

في هذه الدراسة تم استخدام التفاسير الزلزالية الحديثة مثل السمات الزلزالية وتكاملها مع التحليل الطيفي لتوصيف خزان ابولونيا الكربوني تركيبيا وصخريا حيث تم دراسة توزيع التراكيب الجيولوجية المؤثرة في المنطقة محل الدراسة كذلك تقييم حدود الوحدات الجيولوجية ذات الصفات الطيفية الواحدة لمعرفة التوزيع الجيولوجي لصخر الخزان لتحديد المناطق ذات الأهمية في الاستكشاف والتنمية حدد السمات الزلزالية التقليدية، مثل سعة جذر متوسط التربيع وخصائص الطاقة، العيوب الدقيقة في باطن الأرض، ولكنها لا تستطيع الكشف عن التركيب الصخري المحتمل للمكمن. ومع ذلك، تُستخدم تقنيات التحليل الطيفي لتحويل فورييه الأمامي لتحديد توزيعات المكمن وبنيته بدقة، وإبراز شذوذ المسطحات الغازية التي تُقدم مؤشرات واعدة لاستكشاف وتطوير الهيدروكربونات مستقبلًا حيث تم ترتيب 5 مناطق تنازليا حسب الأهمية وكانت أكثر المناطق أهمية هي المنطقة رقم 5 ثم 1 ثم 2 ثم 4 ثم 3.